

# In Silico Screening and In Vitro Validation of Natural-Based LuxS Inhibitors <sup>†</sup>

Susana Fernandes <sup>1,2</sup>, Anabela Borges <sup>1,2</sup>, Inês B. Gomes <sup>1,2</sup>, Sérgio F. Sousa <sup>3</sup> and Manuel Simões <sup>1,2,\*</sup>

<sup>1</sup> LEPABE—Laboratory for Process Engineering, Environment, Biotechnology and Energy, Faculty of Engineering, University of Porto, Rua Dr. Roberto Frias, 4200-465 Porto, Portugal; [up201304637@edu.fe.up.pt](mailto:up201304637@edu.fe.up.pt) (S.F.); [apborges@fe.up.pt](mailto:apborges@fe.up.pt) (A.B.); [ibgomes@fe.up.pt](mailto:ibgomes@fe.up.pt) (I.B.G.)

<sup>2</sup> ALiCE—Associate Laboratory in Chemical Engineering, Faculty of Engineering, University of Porto, Rua Dr. Roberto Frias, 4200-465 Porto, Portugal

<sup>3</sup> UCIBIO/REQUIMTE, BioSIM, Departamento de Biomedicina, Faculdade de Medicina da Universidade do Porto, Alameda Prof. Hernâni Monteiro, 4200-319 Porto, Portugal; [sergiofsousa@med.up.pt](mailto:sergiofsousa@med.up.pt)

\* Correspondence: [mvs@fe.up.pt](mailto:mvs@fe.up.pt)

<sup>†</sup> Presented at the 2nd International Electronic Conference on Antibiotics—Drugs for Superbugs: Antibiotic Discovery, Modes of Action and Mechanisms of Resistance, online, 15–30 June 2022.

**Abstract:** Quorum sensing (QS) inhibitors have emerged as a promising strategy for biofilm control and virulence attenuation, which improves the potential of antimicrobial treatments by increasing microbial susceptibility. The interspecies communication is mediated by autoinducer-2 (AI-2) that is catalyzed by LuxS from S-ribosylhomocysteine (RHC). This study aimed to identify new active phytochemicals against LuxS through in silico analysis, followed by in vitro validation. A representative strain for the study of LuxS inhibition, *Bacillus subtilis*, and a reporter strain sensitive to AI-2, *Vibrio harveyi* BB170, were used. Based on the binding energy scores and compounds cost, the most promising/selected phytochemicals were curcumin (CUR), pioglitazone hydrochloride (PH), and 10-undecenoic acid (UA). In vitro analysis corroborated the QS inhibitory activity of CUR and UA, however, PH had no relevant effect. CUR (at 1.25–5 µg/mL) triggered 33–77% reduction of AI-2 accumulation and UA (at 12.5–50 µg/mL) reduced 36–64%. In conclusion, in silico analysis allowed the identification of LuxS antagonistic phytochemicals, revealing CUR and UA as active QS inhibitors.

**Keywords:** curcumin; molecular docking; phytochemical; pioglitazone hydrochloride; 10-undecenoic acid; virtual screening

**Citation:** Fernandes, S.; Borges, A.; Gomes, I.B.; Sousa, S.F.; Simões, M. In Silico Screening and In Vitro Validation of Natural-Based LuxS Inhibitors. *Med. Sci. Forum* **2022**, *2*, x. <https://doi.org/10.3390/xxxxx>

Academic Editor(s):

Published: date

**Publisher's Note:** MDPI stays neutral with regard to jurisdictional claims in published maps and institutional affiliations.



**Copyright:** © 2022 by the authors. Submitted for possible open access publication under the terms and conditions of the Creative Commons Attribution (CC BY) license (<https://creativecommons.org/licenses/by/4.0/>).

## 1. Introduction

Quorum sensing (QS) is a cell-to-cell signaling process used to regulate gene expression as a function of population density. The mechanism involves the production and release of small chemical molecules, known as autoinducers (AIs), and cell response to AIs level. Above a minimum threshold level, AIs are recognized by specific receptors, which start a signal transduction cascade or repression of target genes, resulting in population-wide changes in phenotype. Examples of processes controlled by QS are virulence expression, motility, symbiosis and biofilm formation, which in turn result in an increased bacterial resistance to antimicrobial agents and pathogenicity [1].

Based on the difference in AI molecules, QS system is classified into four types. One of them is LuxS/AI-2 QS system used for interspecies communication [2]. LuxS catalysis the formation of 4,5-dihydroxy-2,3-pentanedione (DPD) and homocysteine (HCS) from S-ribosylhomocysteine (RHC). DPD is unstable and spontaneously cyclizes to form a furanosyl-borate-diester (AI-2). At high population density, AI-2 is recognized by a specific transmembrane receptor/sensor complex that regulates phosphorylation signal

transduction cascade, activating the expression of related virulence genes [3]. In fact, several bacteria have been identified as able to produce and/or recognize AI-2 [4].

Several authors have demonstrated that the attenuation of the expression of virulence factors and the prevention of the biofilm formation can occur by interference with QS system [5]. In this way, there are a lot of phytochemicals (compounds from the secondary metabolism of plants) that have already been identified as QS inhibitors [6]. This study aims to select new active phytochemicals against LuxS/AI-2 QS of *Bacillus subtilis* using in silico analysis. For that, molecular docking and virtual screening were optimized and applied to screen thousands of phytochemicals (only drug-like compounds) and pick the most potential ones to be in vitro validated, using a reporter strain sensitive to AI-2.

## 2. Materials and Methods

### 2.1. Molecular Docking and Virtual Screening

#### 2.1.1. Protein-Ligand Docking Protocol Validation

Protein Data Bank (PDB) was searched for “LuxS” from *B. subtilis*. For protein-ligand docking protocol validation, a total of seven X-ray crystallographic protein structures and five ligands were retrieved (Table 1). Re-docking of ligands for which there was ligand-target crystallographic structure was performed with AutoDock VINA, GOLD (ChemPLP, GoldScore, ChemScore and ASP), and LeDock. For each software, docking protocol was adjusted to reproduce the known experimental binding poses for each target (minimum Root Mean Square Deviation–RMSD). Cross-docking of ligands was performed to assess the ability of each structure to correctly accommodate ligands from other structures and measure its general usefulness. The average binding energy score from each scoring function for all ligands was calculated for each target protein.

**Table 1.** Available structures of LuxS on PDB.

PDB Code	Resolution (Å)	Ligand
1J98	1.20	--
1IE0	1.60	--
2FQT	1.79	H1D <sup>1</sup>
2FQO	1.87	HYI <sup>2</sup>
1JQW	2.30	HCS
1JVI	2.20	RHC
1YCL	1.80	KRI <sup>3</sup>

<sup>1</sup> (2S)-2-Amino-4-[(2R,3S)-2,3-dihydroxy-3-N-hydroxycarbonyl-propylmercapto]butyric acid. <sup>2</sup> (2S)-2-amino-4-[(2R,3R)-2,3-dihydroxy-3-N-hydroxycarbonyl-propylmercapto]butyric acid. <sup>3</sup> 2-ketone intermediate.

#### 2.1.2. Virtual Screening Protocol Validation

The ChEMBL database (<https://www.ebi.ac.uk/chembl>) was searched for active compounds against LuxS (with known experimental activity), reporting 16 distinct molecules. Decoys are compounds randomly generated with similar 1D physicochemical properties to actives, but distinct 2D topology to be likely non-binders. For all active compounds, the Directory of Useful Decoys Enhanced (<http://dude.docking.org/>) generated a total of 788 distinct decoys. The performance of different scoring functions in discriminating between active compounds and decoys was evaluated by the area under (AU) Receiver Operator Characteristic (ROC) curve and the enrichment factor at 1% (EF1%) and 20% (EF20%) from the ranked lists of active/decoys based on binding energy scores. AU-ROC curve is the plot of the true positive rate (TPR = TP/P) versus false positive rate (FPR = FP/N), where TP is the number of true positives, FP is the number of false positives, P and N are the total number of positives (active compounds) and negatives (decoys), respectively. EF1% and EF20% correspond to the measured number of active ligands recovered at 1% and

20% of the active/decoys database, respectively, over the expected number of recovered active compounds using random scores. At the end of this stage, an optimized virtual screening protocol was selected using the best performing molecular docking software/scoring function and protein structures.

### 2.1.3. Virtual Screening for the Identification of Potential QS Inhibitors

The phytochemical database was developed by combining several online libraries: Analyticon (3608 compounds—<https://ac-discovery.com/>), Molport (1476 compounds—<https://www.molport.com/shop/index>), and PhytoHub (1674 compounds—<http://phytohub.eu/>). After the removal of duplicates and selection of compounds with specific properties associated with other drug-like compounds (Rule of Five), the phytochemical database comprised about 3479 compounds. The previously optimized virtual screening was used to rank and evaluate the binding energy scores of phytochemicals in LuxS.

Curcumin (CUR), 95% (total curcuminoid content), from Turmeric rhizome (Alfa Aesar, Germany), pioglitazone hydrochloride (PH), 98% (Alfa Aesar, China), and 10-undecenoic acid (UA), 99% (Alfa Aesar, Germany) were selected for following in vitro validation. Phytochemical solutions were freshly prepared in 100% DMSO and the final concentration of DMSO used was 6% (*v/v*).

### 2.3. Effects on LuxS/AI-2 QS System

The inhibition of LuxS of *B. subtilis* in presence of selected phytochemicals was measured by the reporter strain *Vibrio harveyi* BB170 (ATCC BAA-1117) according to Bassler, et al. [4] and Taga and Xavier [7] with some modifications. Briefly, *B. subtilis* (Ehrenberg) Cohn (ATCC 6051) was cultured aerobically in Luria-Bertani (LB, Sigma-Aldrich, USA) broth for 14 h at 30 °C (160 rpm). Afterwards, 5 mL of overnight culture was added to 95 mL of sterile LB with a phytochemical solution at different concentrations and grown at 30 °C with agitation. Control samples were performed with DMSO instead of phytochemical solutions. (Z)-4-bromo-5-(bromomethylene)-2(5H)-furanone (furanone C-30, FUR, Sigma-Aldrich, Switzerland) at 1 µM (in DMSO) was used as a positive control. The bacterial growth was monitored by the measure of Abs<sub>610 nm</sub> (spectrophotometer V-1200, VWR, China). After 4.5 h of incubation, the suspension was centrifuged (2000× g, 5 min) and 1 mL aliquots of the cell-free supernatant were collected and filtered [using cellulose acetate syringe filter with a pore size of 0.22 µm (Whatman, VWR, Portugal)]. For AI-2 measurement, *V. harveyi* BB170 was used as reporter strain according to Bassler, et al. [4] and Taga and Xavier [7].

### 2.4. Statistical Analysis

Computational data from the molecular docking and virtual screening studies were analysed using the average and standard deviation (SD) tools of Microsoft Excel. Experimental data were analysed using Dunnett's multiple comparisons test and Tukey's multiple comparisons test from the statistical program GraphPad Prism 6.0 for Windows (GraphPad software, La Jolla, CA, USA). The mean and SD within samples were calculated for all conditions. Statistical differences were established for a probability level of 5% ( $p < 0.05$ ).

## 3. Results and Discussion

### 3.1. Molecular Docking and Virtual Screening Protocol Validation

Molecular docking and virtual screening allowed to recognize potential QS inhibitors from a large phytochemical database that would remain unexploited without it. Although incorrect recognition of false positives or false negatives, this approach is faster and showed higher accuracy than if it was done by traditional methods [8]. This study focused on the optimization/validation of a virtual screening protocol to pick out phytochemicals

with potential QS inhibitory activity against LuxS/AI-2 QS of *B. subtilis*, followed by its in vitro validation.

Assuming a cut-off value for the RMSD between docked and crystallographic ligand poses around 2 Å, all molecular docking software/scoring functions showed good performance in re-docking ligands, except for 1JQW/HCS (Table 2). Additionally, ChemPLP was the docking software/scoring function with the worst overall RMSD (7.28 Å). In this specific case, checking the poses by visual inspection revealed an inverted ligand pose for the lowest binding energy as a result of the chemical interaction of metal ion (zinc) and the terminal carboxy group of both ligands. LeDock was the best performing docking software/scoring function with an average of RMSD of 0.81 Å.

**Table 2.** Re-docking RMSD (Å) values between docked and crystallographic ligand pose for each specific target protein structure for different molecular docking software/scoring functions (VINA, ChemPLP, GOLDScore, ChemScore, ASP, and LeDock).

Receptor	Ligand	VINA	ChemPLP	GoldScore	ChemScore	ASP	LeDock
1JVI	RHC	0.94	6.69	7.15	1.14	1.04	0.84
1YCL	KRI	1.68	7.56	1.02	1.02	0.92	0.68
1JQW	HCS	6.53	7.64	7.78	7.67	0.46	0.54
2FQT	H1D	1.98	6.76	2.07	2.02	2.69	1.72
2FQO	HYI	1.74	7.74	1.36	1.76	2.97	0.29
<b>Average*</b>		1.6 ± 0.4	7.2 ± 0.5	2.9 ± 2.5	1.5 ± 0.4	1.9 ± 0.9	0.9 ± 0.5

\* Re-docking RMSD values for 1JQW/HCS were not included in the average ± SD calculations.

From cross-docking of five ligands using different molecular docking software/scoring functions, the average binding energy score was recovered for each target protein structure (Table 3). The LuxS protein structure 1IE0 showed the worst performance for all ligands using all molecular docking software/scoring functions. The best results, with high binding energy scores, were obtained using ChemPLP, followed by GoldScore, LeDock, and VINA. Results of re-docking and cross-docking suggested 1YCL and 2FQT as the best performing LuxS structures for the conducted analysis.

**Table 3.** Average of binding energy scores of ligands for each LuxS structure using different molecular docking software/scoring functions (VINA, ChemPLP, GOLDScore, ChemScore, ASP, and LeDock).

Receptor	VINA	ChemPLP	GoldScore	ChemScore	ASP	LeDock
1IE0	-0.08 ± 0.08	27 ± 3	35 ± 5	5 ± 3	4 ± 3	-3.8 ± 0.4
1J98	-7.0 ± 0.2	80 ± 3	74 ± 2	24 ± 5	31 ± 0.7	-7.9 ± 0.2
1JVI	-7.4 ± 0.3	78 ± 3	78 ± 3	29 ± 3	33 ± 0.8	-8.2 ± 0.3
1YCL	-7.3 ± 0.2	85 ± 4	81 ± 2	36 ± 1	34 ± 1	-7 ± 2
1JQW	-6.5 ± 0.4	72 ± 3	77 ± 3	27 ± 2	31 ± 0.6	-7.5 ± 0.2
2FQT	-7.0 ± 0.3	85 ± 4	79 ± 4	29 ± 2	31 ± 0.7	-7.8 ± 2
2FQO	-7.1 ± 0.2	81 ± 4	75 ± 2	30 ± 3	32 ± 0.3	-8.0 ± 0.2
<b>Average*</b>	-6.6 ± 1.0	75 ± 11	72 ± 10	28 ± 5	29 ± 6	-7.1 ± 1.5

\* Biding energy scores of ligands for 1IE0 were not included in the average ± SD calculations.

Virtual screening of active/decoys database was performed for 1YCL and 2FQT (the best performing LuxS structures from re-docking and cross-docking analysis), and different statistical tools were used to compare the performance of molecular docking software/scoring functions to give a ranked list of active/decoys—Table 4. VINA, ASP, and LeDock failed to identify positive actives in 1% of active/decoys database. The same tendency was obtained in terms of the recognition metrics at 20%. ChemPLP was evaluated as the best molecular docking software/scoring function for virtual screening of phytochemical database (high EF1% and AU-ROC = 94–96). Although the highest RMSD values,

it was considered non-limiting since ChemPLP had the best performance in discriminating active from decoys and high binding energy scores.

**Table 4.** Performance of molecular docking software/scoring functions (VINA, ChemPLP, GOLD-Score, ChemScore, ASP, and LeDock) in the discrimination between active and decoys for 1YCL and 2FQT structures.

		VINA	ChemPLP	GoldScore	ChemScore	ASP	LeDock
1YCL	EF1%	0.00	31.3	12.6	12.6	0.00	0.00
	EF20%	0.94	4.70	4.40	3.45	0.31	2.20
	AU-ROC	63.7	94.0	87.9	85.4	62.0	68.5
2FQT	EF1%	0.00	18.8	6.27	6.27	0.00	0.00
	EF20%	0.31	4.70	4.39	2.51	0.31	1.26
	AU-ROC	59.8	96.2	87.8	81.0	53.8	61.7

### 3.2. Virtual Screening of Phytochemical Database

Virtual screening using ChemPLP was performed using a phytochemical database to screen potential QS inhibitors against LuxS of *B. subtilis*. Phytochemicals were selected based on high binding energy score, high availability, and low cost. Among the top 10 phytochemicals for both protein structures (1YCL and 2FQT), UA was identified as a potential QS inhibitor. CUR and PH were identified among the top 500. Selected phytochemicals showed binding energy scores close to RHC (natural ligand), indicating favourable chemical interaction. The following in vitro analyses were performed to confirm if revealed phytochemicals had effectively QS inhibition against LuxS/AI-2 QS of *B. subtilis*.

### 3.3. Effects of Phytochemicals on LuxS Inhibition

Based on AI-2 measurement, relative AI-2 reduction (%) in the presence of phytochemicals was determined in comparison to the control sample (*B. subtilis* culture without phytochemicals)—Figure 1. PH did not cause a relevant reduction of AI-2 accumulation in cultures (<15%). On the other hand, CUR and UA caused a significant AI-2 reduction at the tested concentrations. The best phytochemicals against LuxS/AI-2 QS were CUR followed by UA with relative AI-2 reduction ranging between 33–77% and 36–64%, respectively. Both phytochemicals caused greater QS inhibition than positive control (27%).

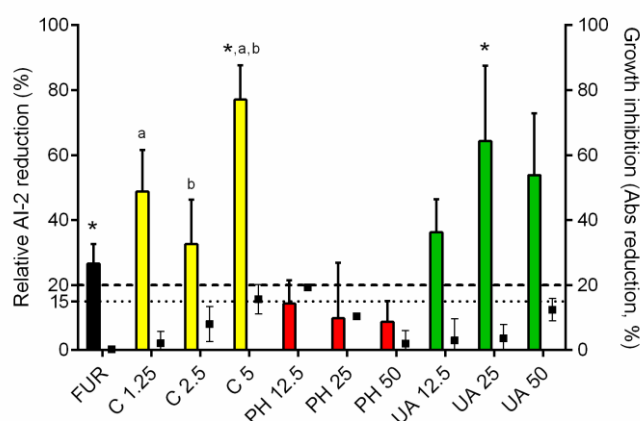


**Figure 1.** Relative AI-2 reduction of *B. subtilis* cultures in the presence of the selected phytochemicals—curcumin (CUR), pioglitazone hydrochloride (PH), and 10-undecenoic acid (UA) at different concentrations (in  $\mu\text{g/mL}$ ) (left-y axis; bars). Effects on cell density as  $\text{Abs}_{610\text{ nm}}$  reduction (right-y axis; dots). Positive control corresponded to relative AI-2 reduction on the culture in the presence of furanone C-30 (FUR). Dashed lines correspond to cut-off values for the maximum growth inhibition (20% of absorbance) and for minimum QS inhibition (15%). \*—Relative AI-2 reduction in presence of phytochemicals was statistically different from FUR (Dunnett's multiple comparisons test,

$p < 0.05$ ). <sup>a</sup> and <sup>b</sup>—AI-2 accumulation was statistically different between different concentrations of each phytochemical (Tukey's multiple comparisons test,  $p < 0.05$ ). Values are the means  $\pm$  SDs of three independent experiments.

Phytochemicals have been identified as potential LuxS/AI-2 QS inhibitors. For instance, the QS inhibition promoted by CUR was also demonstrated against *Streptococcus mutants* [9]. To the best authors' knowledge, this study was the first to demonstrate the QS inhibition by UA. However, previous research identified several long-chain fatty acids as LuxS/AI-2 QS inhibitors [10]. In addition, it was demonstrated that agaric acid (another fatty acid) cause QS inhibition against *Salmonella*, inhibiting biofilm formation through reduction of flagellar motility [11].

#### 4. Conclusions

The optimized virtual screening protocol permitted at some extent a reliable identification of new potential QS inhibitors from a phytochemical drug-like database against LuxS. As the QS mechanism is involved in biofilm formation and virulence expression, QS inhibition can effectively be used to improve antimicrobial treatments outcomes by increasing microbial susceptibility and diminishing infectivity. In silico analysis revealed CUR, PH, and UA as potential QS inhibitors. In vitro assays corroborated the QS inhibitory activity using CUR (at 1.25–200  $\mu\text{g/mL}$ ) and UA (at 12.5–250  $\mu\text{g/mL}$ ), however, PH had no relevant effect. This study demonstrated the power of molecular docking/virtual screening methodology in the prediction of potential chemical interactions between ligands and the selected targets.

**Author Contributions:** Conceptualization, S.F., A.B., I.B.G., S.F.S., and M.S.; methodology, S.F., A.B., I.B.G., S.F.S., and M.S.; software, S.F.S.; validation, S.F.; formal analysis, S.F.; investigation, S.F.; resources, S.F.S. and M.S.; data curation, S.F.; writing—original draft preparation, S.F.; writing—review and editing, A.B., I.B.G., S.F.S., and M.S.; supervision, S.F.S. and M.S.; project administration, M.S.; funding acquisition, M.S. All authors have read and agreed to the published version of the manuscript.

**Funding:** This work was financially supported by: LA/P/0045/2020 (ALiCE), UIDB/00511/2020 and UIDP/00511/2020 (LEPABE), funded by national funds through FCT/MCTES (PIDDAC); Projects PTDC/BIBTI/30219/2017—POCI-01-0145-FEDER-030219, POCI-01-145-FEDER-006939, POCI-01-0247-FEDER035234, POCI-01-0247-FEDER-072237, funded by FEDER funds through COMPETE2020—Programa Operacional Competitividade e Internacionalização (POCI) and by national funds (PIDDAC) through FCT/MCTES; national funds from Fundação para a Ciência e a Tecnologia (grant numbers: UIDP/04378/2020, UIDB/04378/2020, and 2020.01423.CEECIND/CP1596/CT0003); Project HealthyWaters (NORTE-01-0145-FEDER000069), supported by Norte Portugal Regional Operational Programme (NORTE 2020) under the PORTUGAL 2020 Partnership Agreement through the European Regional Development Fund (ERDF), and by the FCT PhD scholarship attributed to Susana Fernandes (FCT/SFRH/BD/147276/2019). Anabela Borges thanks the FCT for the financial support of her work contract through the Scientific Employment Stimulus—Individual Call—[CEECIND/01261/2017].

**Institutional Review Board Statement:** Not applicable.

**Informed Consent Statement:** Not applicable.

**Data Availability Statement:** Not applicable.

**Conflicts of Interest:** The authors declare no conflict of interest.

#### References

1. Brindhadevi, K.; LewisOscar, F.; Mylonakis, E.; Shanmugam, S.; Verma, T.N.; Pugazhendhi, A. Biofilm and quorum sensing mediated pathogenicity in *Pseudomonas aeruginosa*. *Process Biochem.* **2020**, *96*, 49–57. <https://doi.org/10.1016/j.procbio.2020.06.001>.
2. Zhang, B.; Ku, X.; Zhang, X.; Zhang, Y.; Chen, G.; Chen, F.; Zeng, W.; Li, J.; Zhu, L.; He, Q. The AI-2/luxS quorum sensing system affects the growth characteristics, biofilm formation, and virulence of *Haemophilus parasuis*. *Front. Cell Infect. Microbiol.* **2019**, *9*, 62. <https://doi.org/10.3389/fcimb.2019.00062>.

3. Guo, M.; Gamby, S.; Zheng, Y.; Sintim, H.O. Small molecule inhibitors of AI-2 signaling in bacteria: state-of-the-art and future perspectives for anti-quorum sensing agents. *Int. J. Mol. Sci.* **2013**, *14*, 17694–17728. <https://doi.org/10.3390/ijms140917694>.
4. Bassler, B.L.; Greenberg, E.P.; Stevens, A.M. Cross-species induction of luminescence in the quorum-sensing bacterium *Vibrio harveyi*. *J. Bacteriol.* **1997**, *179*, 4043–4045. <https://doi.org/10.1128/jb.179.12.4043-4045.1997>.
5. Paluch, E.; Rewak-Soroczynska, J.; Jedrusik, I.; Mazurkiewicz, E.; Jermakow, K. Prevention of biofilm formation by quorum quenching. *Appl. Microbiol. Biotechnol.* **2020**, *104*, 1871–1881. <https://doi.org/10.1007/s00253-020-10349-w>.
6. Mishra, R.; Panda, A.K.; De Mandal, S.; Shakeel, M.; Bisht, S.S.; Khan, J. Natural anti-biofilm agents: strategies to control biofilm-forming pathogens. *Front. Microbiol.* **2020**, *11*, 566325. <https://doi.org/10.3389/fmicb.2020.566325>.
7. Taga, M.E.; Xavier, K.B. Methods for analysis of bacterial autoinducer-2 production. In *Current Protocols in Microbiology*; Wiley Online Library: Hoboken, NJ, USA, 2011; Unit 1C.1. <https://doi.org/10.1002/9780471729259.mc01c01s23>.
8. Puertas-Martin, S.; Banegas-Luna, A.J.; Paredes-Ramos, M.; Redondo, J.L.; Ortigosa, P.M.; Brovarets, O.O.; Perez-Sanchez, H. Is high performance computing a requirement for novel drug discovery and how will this impact academic efforts? *Expert Opin. Drug Discov.* **2020**, *15*, 981–986. <https://doi.org/10.1080/17460441.2020.1758664>.
9. Li, X.; Yin, L.; Ramage, G.; Li, B.; Tao, Y.; Zhi, Q.; Lin, H.; Zhou, Y. Assessing the impact of curcumin on dual-species biofilms by *Streptococcus mutans* and *Candida albicans*. *MicrobiologyOpen* **2019**, *8*, e937. <https://doi.org/10.1002/mbo3.937>.
10. Widmer, K.W.; Soni, K.A.; Hume, M.E.; Beier, R.C.; Jesudhasan, P.; Pillai, S.D. Identification of poultry meat-derived fatty acids functioning as quorum sensing signal inhibitors to autoinducer-2 (AI-2). *J. Food Sci.* **2007**, *72*, M363–M368. <https://doi.org/10.1111/j.1750-3841.2007.00527.x>.
11. Lories, B.; Belpaire, T.E.R.; Yssel, A.; Ramon, H.; Steenackers, H.P. Agaric acid reduces *Salmonella* biofilm formation by inhibiting flagellar motility. *Biofilm* **2020**, *2*, 100022. <https://doi.org/10.1016/j.biofilm.2020.100022>.